JOURNAL OF GEOPHYSICAL RESEARCH, VOL. 111, D12312, doi:10.1029/2005JD006744, 2006

Decreases in stratospheric water vapor after 2001: Links to changes in the tropical tropopause and the Brewer-Dobson circulation

William J. Randel,[1] Fei Wu,[1] Holger Vömel,[2] Gerald E. Nedoluha,[3] and Piers Forster[4]

Received 6 October 2005; revised 18 January 2006; accepted 20 March 2006; published 27 June 2006.

[1] Time series of stratospheric water vapor measurements by satellites and balloons show persistent low values beginning in 2001. Temperature observations show that the tropical tropopause has been anomalously cold during this period, and the observed water vapor changes (approximately −0.4 ppmv) are consistent with the temperature decreases (approximately −1 K). The cold anomalies occur in the tropics over a narrow vertical layer near 15–20 km. There have been corresponding changes in the tropical ozone profile over the same period, with ∼10% reductions over a similar narrow layer near the tropopause. The variations in temperature and ozone appear coupled, and the spatial patterns of the changes since 2001 are consistent with an increase in the mean tropical upwelling (Brewer-Dobson) circulation. Estimates of tropical upwelling derived from eddy statistics (''downward control'') show coherence with interannual temperature changes, including a consistent increase after 2001. Part of the temperature changes may also be explained as a radiative response to the observed ozone decreases. The results paint a consistent picture of enhanced tropical upwelling after 2001, resulting in colder temperatures, lower water vapor and lower ozone near the tropical tropopause. The recent low values significantly influence estimates of decadal-scale trends in temperature and ozone near the tropical tropopause.

Citation: Randel, W. J., F. Wu, H. Vömel, G. E. Nedoluha, and P. Forster (2006), Decreases in stratospheric water vapor after 2001: Links to changes in the tropical tropopause and the Brewer-Dobson circulation, *J. Geophys. Res.*, *111*, D12312, doi:10.1029/2005JD006744.

1. Introduction

[2] Stratospheric water vapor provides the most direct evidence that air enters the stratosphere primarily in the tropics. Both the overall dryness of the stratosphere [*Brewer*, 1949] and the large annual cycle in stratospheric water vapor [*Mote et al.*, 1996] are evidence that air passes the cold tropical tropopause in transit to the stratosphere. Recent calculations show that the observed annual cycle in water vapor is in quantitative agreement with transport across the seasonally varying tropopause [*Fueglistaler et al.*, 2005]. Interannual changes in stratospheric water vapor also reflect variations in tropopause temperatures; the temperature effects of the stratospheric quasi-biennial oscillation (QBO) and the El Niño–Southern Oscillation (ENSO) are seen in stratospheric water vapor in both observations [*Randel et al.*, 2004, hereinafter referred to as R04] and model calculations [*Giorgetta and Bengston*, 1999; *Geller et al.*, 2002; *Fueglistaler and Haynes*, 2005]. Because of this relationship, stratospheric water vapor may be a sensitive indicator of variations in tropical tropopause temperatures.

[3] The Halogen Occultation Experiment (HALOE) satellite instrument [*Russell et al.*, 1993] has been making near-global measurements of stratospheric water vapor since late 1991. Continuing observations from HALOE show a substantial and persistent decrease in stratospheric water vapor beginning in approximately 2001, and continuing to present. This change in water vapor is also observed in several other satellite and balloon data sets. The focus of this paper is to explore variations in tropical tropopause behavior as an explanation for the recent low water vapor values. We examine tropopause temperatures to quantify coherence with water vapor, and isolate the spatial structure of recent temperature changes. We also examine variations in ozone profile near the tropical tropopause based on balloon and satellite data sets, and find ozone decreases after 2001 that have similar space-time characteristics to the observed temperature changes. One mechanism for such coupled temperature and ozone changes could be an increase in the mean upwelling (Brewer-Dobson) circulation near the tropical tropopause (here vertical advection is a dominant term in the thermodynamic and ozone continuity equations, and coherent temperature-ozone changes result from similarly signed vertical gradients in potential temperature and ozone). Accordingly, we examine circulation statistics of derived tropical upwelling to search for changes consistent with the tropical temperature and ozone decreases

[1] National Center for Atmospheric Research, Boulder, Colorado, USA.
[2] Global Monitoring Division, NOAA Earth System Research Laboratory, Boulder, Colorado, USA.
[3] Naval Research Laboratory, Washington, D. C., USA.
[4] School of Earth and Environment, University of Leeds, Leeds, UK.

0148-0227/06/2005JD006744$09.00

after 2001. Another mechanism for coupled temperature and ozone variations is a simple radiative response of temperature to ozone changes, and we used idealized model calculations to estimate the importance of this effect. We also examine longer-term variations in tropical tropopause temperatures and ozone, to put the recent changes in the context of decadal-scale variability.

2. Data

2.1. Stratospheric Water Vapor

[4] The HALOE instrument provides high-quality vertical profiles of stratospheric water vapor derived from solar occultation measurements [*Russell et al.*, 1993; *Harries et al.*, 1996]. HALOE began operating in October 1991, with data analyzed here through August 2005. We use the v19 retrieval product obtained in so-called level 3 format. The HALOE measurements extend from the approximate local tropopause level to about 80 km; the vertical resolution is ~2 km, but the level 3 data are slightly oversampled with a 1.3 km vertical spacing (12 standard levels per decade of pressure, namely 100., 82.5, 68.1,. . .hPa). HALOE water vapor signals have been extremely stable throughout more than 13 years of observations. There is no trend in the absolute signal which has only changed by 0.5% since launch and there is no effect due to instrument drift because the basic signal used for retrieval is a ratio measurement that will remove any bias shifts (J. M. Russell III, Hampton University, private communication, 2005). The HALOE occultation sampling makes approximately 15 sunrise and 15 sunset measurements per day, with sunrises and sunsets usually separated in latitude. The latitudinal sampling progresses in time so that it takes approximately one month to sample the latitude range ~60°N-S. We bin the combined sunrise and sunset data into monthly samples for further analyses.

[5] We briefly examine two other time series of stratospheric water vapor measurements to show that the low values after 2001 are not an artifact of the HALOE data. These data sets include balloon-borne frost point hygrometer measurements from Boulder, Colorado (40°N, 105°W), described by *Oltmans et al.* [2000], and Polar Ozone and Aerosol Measurement III (POAM III) satellite observations, detailed by *Nedoluha et al.* [2002]. The Boulder balloon measurements are made approximately once per month, and sample altitudes ~5–25 km. POAM III is a solar occultation instrument on a polar orbiting satellite, providing measurements only over high latitudes (~55–70°N and ~65–85°S). Variations in lower-stratospheric water vapor over the Arctic are controlled primarily by transport from tropical latitudes [*Nedoluha et al.*, 2002; R04], whereas in situ dehydration dominates over the Antarctic. Our comparisons here focus on the Arctic POAM III measurements, and cover the time period 1998–2005; we omit data from June–August 2004 that have some apparent problems.

2.2. Radiosonde Temperatures

[6] Temperature data used here are from tropical radiosonde measurements, and include results from two different data sets. For examining recent results (over the HALOE time period, 1992–2005) we use data from 30 tropical stations (~25°N–25°S) obtained from the Integrated Global Radiosonde Archive (IGRA) from the NOAA National Climate Data Center; somewhat more attention is focused on a subset of 13 stations close to the equator (over 10°N–10°S). The station locations are shown below. Monthly means have been derived from daily measurements at standard pressure levels, plus the cold point tropopause (temperature minimum). We have compared data from each station with colocated satellite measurements from the Microwave Sounding Unit (MSU), following *Randel and Wu* [2006], to demonstrate that these stations do not have significant data homogeneity problems for the time period after 1992.

[7] Examination of longer-term (decadal) changes in tropical tropopause temperatures requires special attention, because changes (improvements) in radiosonde instrumentation or radiation corrections over time can result in spurious cooling trends [*Seidel et al.*, 2001; *Lanzante et al.*, 2003a, 2003b; *Randel and Wu*, 2006]. Here we briefly examine longer-term changes in tropical tropopause temperatures based on a number of radiosonde stations from the LKS data set [*Lanzante et al.*, 2003a, 2003b], which have undergone adjustments to minimize inhomogenieties. These time series are updated to 2004 using the Integrated Global Radiosonde Archive (IGRA), and the combined data are termed LKS+IGRA. Detailed comparisons with colocated satellite measurements suggest that many of the tropical LKS+IGRA stations still have artificial cooling biases in the lower stratosphere, with magnitudes in excess of 0.5 K/decade [*Randel and Wu*, 2006]. Accordingly, for decadal-scale changes we restrict our attention to a handful of stations where such biases are relatively small; these include Hilo (20°N), San Juan (18°N), Nairobi (1°S), Manaus (3°S), Townsville (19°S) and Rio de Janeiro (23°S).

2.3. Ozone

[8] Time series of tropical ozone profiles are obtained from the SHADOZ (Southern Hemisphere Additional Ozonesondes) data archive at http://croc.gsfc.nasa.gov/shadoz/ [*Thompson et al.*, 2003]. SHADOZ consists of a set of 12 tropical stations with ozonesonde soundings approximately once per month, beginning in 1998. The analyses here focus on data from 7 near-equatorial stations with continuous records that cover the period 1998–2005. These stations include Nairobi, Kuala Lampur, Fiji, Samoa, San Cristobal, Natal and Ascension Island, with locations also shown below.

[9] We also include ozone data from Stratospheric Aerosol and Gas Experiment II (SAGE II) satellite measurements [*McCormick et al.*, 1989]. SAGE II is a solar occultation instrument with similar space-time sampling to HALOE, and made measurements covering late 1984 to the middle of 2005. The vertical resolution of SAGE II is ~0.5–1 km, which is a key attribute for analysis of the tropopause region. We use the version 6.2 retrieval of SAGE II data, covering the period November 1984 to March 2005 (excluding 2 years following the Mt. Pinatubo volcanic eruption in June 1991).

3. Results

3.1. Stratospheric Water Vapor and Tropical Tropopause Temperatures

[10] The evolution of near-global (60°N–60°S) water vapor at 82 hPa for the entire HALOE record (1992–

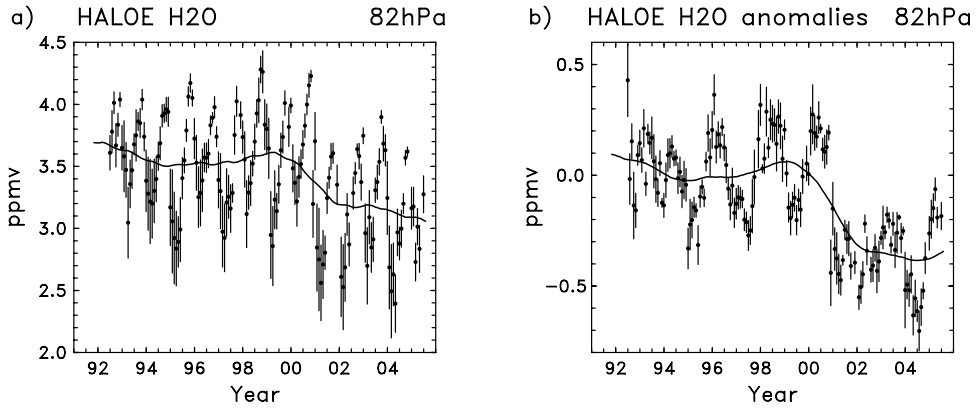

Figure 1. (a) Time series of near-global mean (∼60°N-S) water vapor at 82 hPa derived from HALOE data. The circles show monthly mean values, and error bars denote the monthly standard deviation. (b) Deseasonalized near-global mean H_2O anomalies at 82 hPa. In both panels the solid lines are running Gaussian-weighted means of the individual points (using a Gaussian half width of 12 months).

2005) is shown in Figure 1a. Two features are evident in these data, namely (1) a large annual cycle (∼1 ppmv), which is related to the annual cycle in tropical tropopause temperatures [*Mote et al.*, 1996], and (2) a decrease in overall values (by ∼0.4 ppmv) after approximately 2001. Interannual anomalies are most easily analyzed by removing the annual cycle, and Figure 1b shows a deseasonalized version of the near-global anomalies (the data are deseasonalized using harmonic analysis at each latitude and height, as described by R04). The deseasonalized data show the relatively abrupt drop after ∼2001, persisting to near the present. There is also clear variability on an approximate 2-year timescale, associated with the QBO (discussed in detail by R04 and *Fueglistaler and Haynes* [2005]), and such variability is evident both before and after the 2001 decrease. The interannual variations seen in Figure 1 (both the QBO and recent decrease) are observed to originate in the tropical lower stratosphere, and propagate in latitude to cover most of the global lower stratosphere with a timescale of several months (R04). The tropical anomalies also propagate in altitude at a rate of ∼8 km/year, so that dry anomalies are evident near 10 hPa (32 km) after ∼2003. Figure 2 shows a near-global cross section of water vapor changes for the period 2001–2004, calculated as a difference with respect to the period 1994–2000. While the largest differences (>0.5 ppmv) occur in the tropical lower stratosphere, the overall patterns show truly global changes, with differences of 0.2–0.3 ppmv over most of the stratosphere below 30 km. These decreases represent approximately 5–15% of background values.

[11] The recent low values of stratospheric water vapor are also observed in several other data sets. Figure 3 compares interannual changes derived from HALOE (representing near-global means), Boulder balloon measurements (at a single location near 40°N), and POAM III (Arctic measurements over ∼55–70°N). Each data set shows relatively low values after 2001, albeit with different details depending on the data source. The Boulder balloon measurements suggest a systematic decrease in water vapor after 2001, similar to HALOE, but with substantial variability within the individual measurements. We note that the Boulder time series suggests increasing values prior to ∼1998, which are part of a long-term increase seen in these data [*Oltmans et al.*, 2000]. These increases in Boulder measurements for ∼1992–2000 are substantially different from HALOE data for the same time period (which show no increase), and this difference is not understood at present (see R04). However, of more interest here are the decreases after 2001 observed in both data sets. The relatively shorter POAM III record also shows decreased water vapor in the Arctic lower stratosphere after 2001. As noted in R04, the near-global HALOE sampling shows that these Arctic anomalies originate in tropical latitudes and propagate northward, and direct comparison between POAM III and HALOE anomalies near 60°N shows excellent agreement (to ∼0.2 ppmv; R04). Overall, both the Boulder balloon and POAM III data confirm the recent water vapor decreases observed in HALOE data. *Chiou et al.* [2006] have also shown reasonable agreement between HALOE data and SAGE II water vapor measurements, including relative decreases in both data sets for the period after 1996.

[12] As noted above, seasonal and interannual changes in stratospheric water vapor are tied to variations in tropical

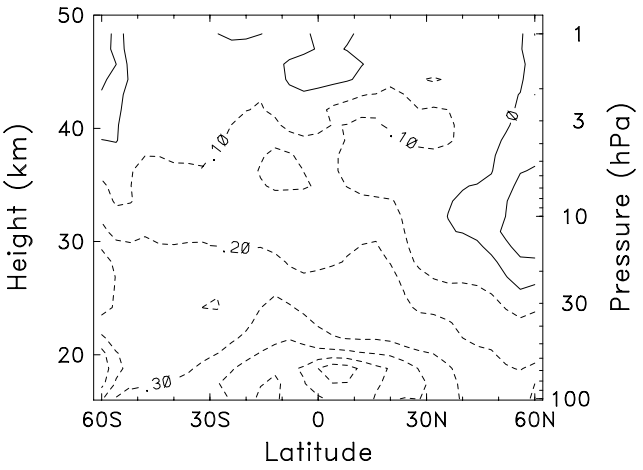

Figure 2. Meridional cross section of HALOE water vapor anomalies for 2001–2004, calculated as a difference from the period 1994–2000. Contour interval is 0.1 ppmv.

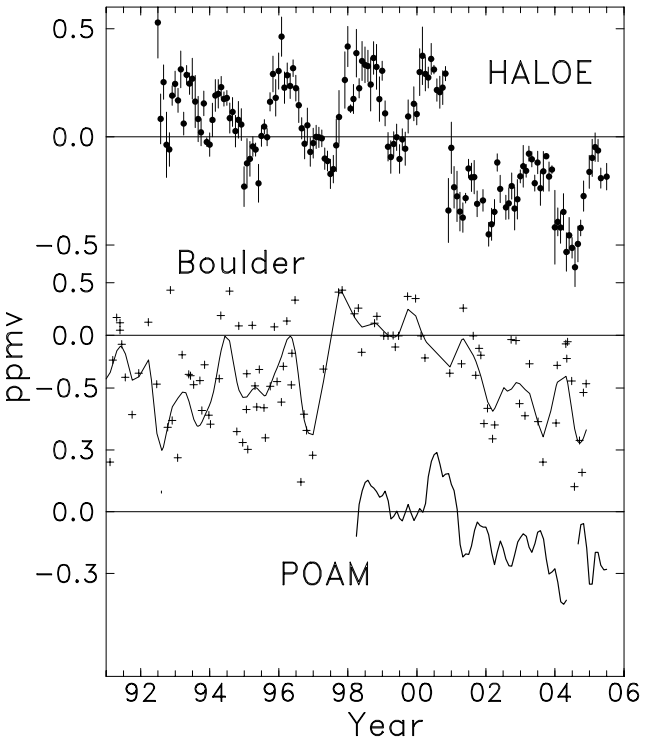

Figure 3. Comparison of lower-stratospheric water vapor anomalies derived from HALOE satellite data; balloon measurements from Boulder, Colorado (40°N); and POAM III satellite measurements. The HALOE data details are the same as in Figure 1b. The plus signs show the individual Boulder balloon measurements (averaged over 16–18 km), and the line is a smooth fit to the time series using a running Gaussian average with half width three months. The POAM III data represent Arctic latitudes (∼55–70°N), are averaged over 16–18 km, and the monthly data have been smoothed with a running 1-2-1 average.

tropopause temperatures. This is seen in the observed correlations between water vapor and tropopause temperature anomalies [R04; *Fueglistaler and Haynes*, 2005], and also in the tropical origin of the dry anomalies, followed by propagation to higher latitudes (R04). Figure 4 shows time series of deseasonalized cold point tropopause anomalies for 1992–2005 derived from radiosonde data for stations over 10°N–10°S, together with the deseasonalized HALOE water vapor anomalies from Figure 1b. The temperature time series in Figure 4 shows similar variability to that for water vapor, including both ∼2-year (QBO) variations and relatively cold anomalies for the period after 2001. The correlation between the temperature and water vapor anomalies in Figure 1 (with water vapor lagged by two months) is 0.73, which is significant above the 1% level. The magnitude of the water vapor changes is consistent with the observed temperatures (R04), and the variations in Figure 4 are also consistent with the empirical relationship derived by *Fueglistaler and Haynes* [2005], with temperature changes of ±1 K near the cold point corresponding to water vapor anomalies of ±0.5 ppmv.

[13] Spatial characteristics of the recent tropopause temperature changes are examined by comparing the period 2001–2004 with the previous 6-year average 1994–2000. The 1994–2000 period allows averaging over approximately 3 QBO cycles, and avoids the tropical stratospheric warming that followed the Mt. Pinatubo volcanic eruption in June 1991, and which lasted for several years [*Angell*, 1997]. Figure 5 shows the vertical profile of temperature differences for 2001–2004 for each of the 13 tropical radiosonde stations over the equatorial band 10°N–10°S, revealing cold anomalies of ∼1 K over a narrow vertical layer centered near the tropopause (∼15–20 km) at each station. There are warm tropospheric temperature anomalies of 0.3–0.5 K at many stations (mainly over the western Pacific Ocean), and these are associated with a relatively weak El Niño occurring during 2002–2004. Figure 6 shows the temperature anomalies for 2001–2004 at the 80 hPa level for each station. Cold anomalies are observed throughout the tropics, with largest values within 10–15° of the equator, and the magnitude of the changes is not strongly dependent on longitude.

3.2. Ozone Changes

[14] The vertical profile of ozone in the tropical lower stratosphere reflects a balance between photochemical production and large-scale upwelling [*Avallone and Prather*, 1996], i.e., $w^* \cdot dO_3/dz \sim P$, where w^* is the upwelling velocity, dO_3/dz is the vertical ozone gradient, and P is photochemical production. Input of low ozone via tropical deep convection also influences the ozone profile, and this appears to be most important over ∼12–14 km, although the influence can reach ∼16 km [*Folkins et al.*, 2002; *Dessler*, 2002; *Solomon et al.*, 2005]. Mixing from extratropics also contributes in the tropical lower stratosphere, above ∼18 km [*Volk et al.*, 1996]. Here we examine tropical ozone changes during recent years in the SHADOZ ozonesonde and SAGE II satellite data sets. SHADOZ began

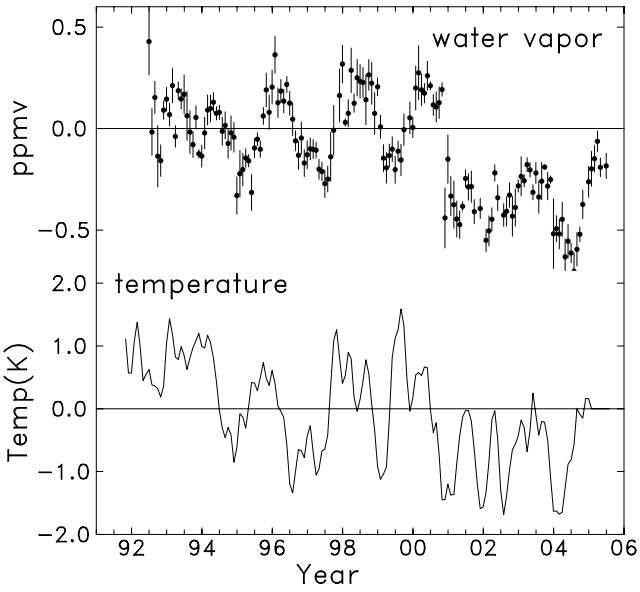

Figure 4. (top) Time series of deseasonalized anomalies in lower-stratospheric (82 hPa) water vapor derived from HALOE data (as in Figure 1b). (bottom) Time series of deseasonalized anomalies in tropical cold point temperature, derived from 14 radiosonde stations over 10°N–10°S.

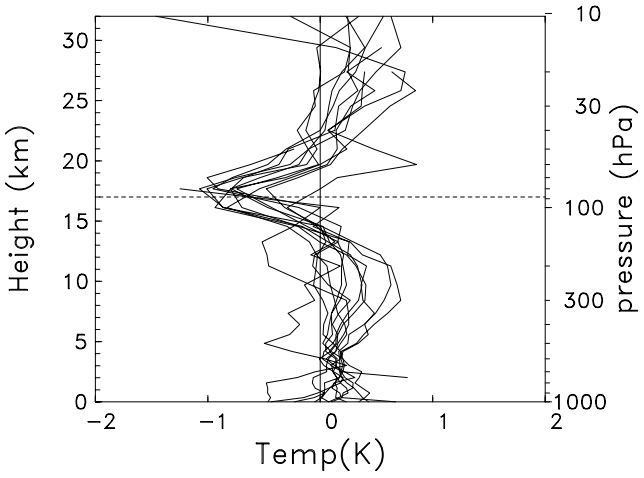

Figure 5. Vertical profile of temperature differences between (2001–2004) and (1994–2000), derived from tropical radiosonde measurements over 10°N–10°S. Individual lines show changes at each station. The dashed line is near the cold point tropopause (17 km).

regular measurements in 1998, and continuous records are available from 7 tropical stations (with location illustrated in Figure 6). There is a large annual cycle in ozone near the tropical tropopause, and we have deseasonalized the SHADOZ and SAGE II using harmonic analysis to study interannual changes. Figure 7 shows time series of deseasonalized ozone anomalies at 16–18 km from SHADOZ data (averaged over the 7 stations), together with similar results from the zonally averaged SAGE II data spanning 1984–2004. The SHADOZ and SAGE II data show reasonably good agreement for ozone variations during the overlap period 1998–2004, and both data sets reveal negative ozone anomalies (of order −10%) covering the years 2001–2004. This timing is similar to the tropopause temperature variations seen in Figure 1. The agreement between SAGE II and SHADOZ anomalies in Figure 7 is remarkable, given the vastly different sampling of the two data sets, and relatively small ozone amounts (∼1–2 ppmv) in this region to begin with.

[15] The vertical profile of ozone anomalies for 2001–2004, expressed as percentage changes compared to the period 1998–2000, is shown for each of the SHADOZ stations in Figure 8, together with corresponding SAGE II results. The SHADOZ data show negative ozone changes of magnitude ∼10–20% in the region near the tropopause, with similar changes observed for 5 of the 7 stations over ∼17–19 km. For a few stations (San Cristobal, Samoa and Fiji), large percentage ozone decreases extend to lower altitudes (∼14 km). Overall smaller ozone decreases are observed for the stations at Natal and Ascension Island, in the south Atlantic region (note Ascension Island also shows small temperature changes in Figure 6). The SAGE II zonal mean results show ozone decreases over ∼15–20 km maximizing near −10%, within the range of results from the individual SHADOZ stations. The latitudinal structure of changes after 2001 derived from SAGE II data (not shown) exhibits largest changes in the tropics, over approximately 20°N-S. Thus the recent ozone changes show space-time patterns very similar to the observed temperature changes, namely persistent negative anomalies since 2001, occurring in a narrow vertical region near the tropical tropopause (∼15–20 km), with changes occurring over most longitudes and centered near the equator.

3.3. Changes in Tropical Upwelling and Subtropical Momentum Balance

[16] The longitudinal, latitudinal and vertical structure of the observed temperature and ozone decreases since 2001 are consistent with an increase in the mean tropical upwelling, i.e., an increase in the stratospheric Brewer-Dobson circulation. Changes in mean upwelling will produce effects that maximize in the deep tropics over a wide range of longitudes. Seasonal timescale increases in upwelling will result in largest temperature changes near and above the tropopause, in a region where the radiative relaxation timescale is long (∼16–20 km); such enhanced temperature response over this altitude range is the cause for the observed large annual cycle in temperature in this region [*Randel et al.*, 2002]. Likewise, the fractional ozone response to tropical upwelling changes is magnified over this same altitude region (∼16–20 km), because this is the region where the background vertical ozone gradient (d ln

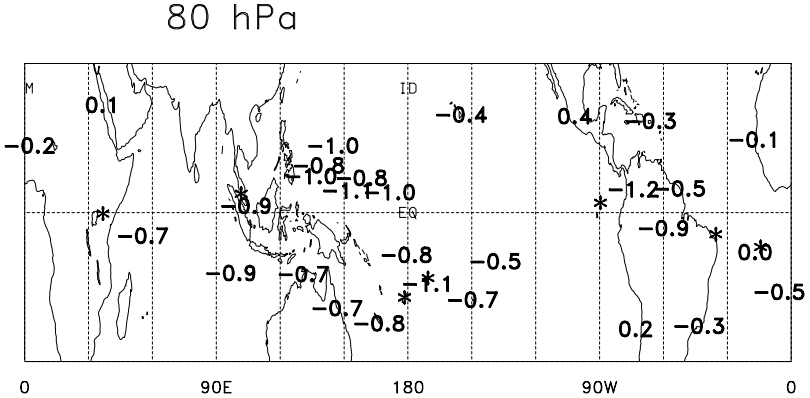

Figure 6. Temperature differences at 80 hPa between the periods (2001–2004) and (1994–2000), at each individual radiosonde station. The asterisks denote the location of the near-equatorial SHADOZ ozonesonde stations.

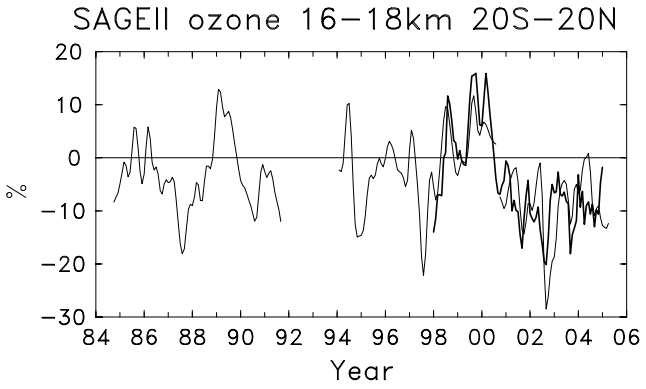

Figure 7. Deseasonalized zonal mean ozone anomalies over 16–18 km and 20°N–20°S (thin lines), derived from SAGE II zonal mean data. Corresponding anomalies calculated from an average of 7 tropical ozonesonde stations from SHADOZ (thick line), covering just 1998–2004.

O_3/dz) is maximum (and where a large annual cycle in ozone is observed). The sign of the temperature and ozone responses to upwelling is the same, on the basis of similarly signed vertical gradients in potential temperature and ozone. Thus the correlated temperature and ozone decreases near the tropopause are consistent with an increase in upwelling, and it makes sense to search for other evidence for an increased upwelling circulation, and in particular a change beginning in 2001.

[17] The global-scale stratospheric Brewer-Dobson circulation is in balance with eddy forcing from large and small-scale waves [*Haynes et al.*, 1991; *Holton et al.*, 1995]. A direct estimate for wave forcing of tropical upwelling is provided by calculation of the zonal mean momentum budget in subtropics, coupled with the continuity equation [*Rosenlof*, 1995; *Plumb and Eluszkiewicz*, 1999; *Randel et al.*, 2002; *Kerr-Munslow and Norton*, 2006]. Using this formalism, tropical upwelling is proportional to the difference in (vertically integrated) EP flux divergence, weighted by the inverse Coriolis parameter, between NH and SH subtropics. In practice the calculations are limited by uncertainties in EP flux estimates near the tropopause in low latitudes (magnified by the inverse Coriolis parameter), and there is a limit to making estimates too close to the equator. Our calculations here are based on details discussed by *Randel et al.* [2002], applied to meteorological fields from NCEP [*Kalnay et al.*, 1996] and ERA40 (see http://www.ecmwf.int/research/era) reanalysis data sets. The derived upwelling is termed $\langle \overline{w}^*_m \rangle$, where the angle brackets denote the average value over a latitude band, and the subscript m denotes that the upwelling is derived from momentum balance [*Randel et al.*, 2002]. We find that reasonable results are obtained for latitude limits of ±20° (and thus the results apply to averaged upwelling over 20°N–20°S). Interannual variations are calculated by removing the (relatively large) seasonal cycle, and Figure 9 shows the resulting interannual anomalies in derived upwelling $\langle \overline{w}^*_m \rangle$ at 100 hPa for 1992–2004, together with observed changes in tropical tropopause temperatures (the same data as in Figure 4). Interannual variations in derived $\langle \overline{w}^*_m \rangle$ are of order ±0.1 mm/s, compared to background values that vary from 0.2 to 0.6 mm/s over the annual cycle. Anomalies in Figure 9 show reasonable agreement between the NCEP and ERA40 data, which gives some confidence in these highly derived statistics (note that the ERA40 data end in 2002). Comparison between the derived $\langle \overline{w}^*_m \rangle$ anomalies and observed tropopause temperature variations in Figure 9 shows substantial correlation, with enhanced upwelling correlated to cold temperatures (the correlation coefficient for NCEP data over 1993–2004 is −0.53, significant at the 1% level). This relationship is reasonable, and suggests that some fraction of interannual variability in tropical tropopause temperature is controlled by zonally averaged momentum balance in the subtropics (near 20°N-S). The more recent period of cold tropopause temperature anomalies after 2001 is associated with positive and somewhat persistent $\langle \overline{w}^*_m \rangle$ anomalies; note that the individual peaks in $\langle \overline{w}^*_m \rangle$ are correlated with cold anomalies during this period. These results paint a consistent picture of enhanced tropical upwelling for the period 2001–2004, resulting in colder temperatures (and associated lower water vapor) and low ozone near the tropical tropopause.

[18] Given the coherent upwelling results in Figure 9, with somewhat enhanced values after 2001, a natural extension is to examine changes in EP flux divergence leading to these anomalies. Figure 10a shows the climatological EP flux divergence patterns derived from NCEP data for 1994–2000, and Figure 10b shows anomalies for the period 2001–2004 (i.e., differences compared to 1994–2000; note that the full field for 2001–2004 (not shown) looks very similar to Figure 10a, as the anomalies are relatively small). While the anomalies are small in Figure 10b, there is clear systematic structure, with enhanced convergence of EP flux in the subtropics of both hemispheres near 20°N and S;

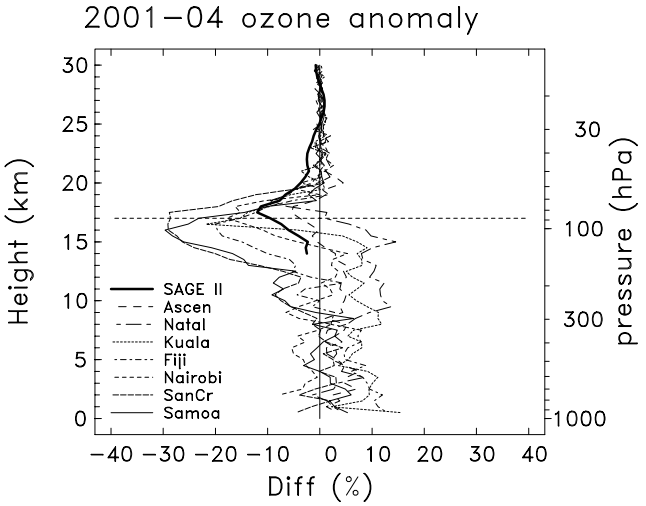

Figure 8. Vertical profile of ozone changes between the periods (2001–2004) and (1998–2000), derived from SHADOZ ozonesonde data. Each line represents the percentage changes for the individual stations, as noted. The thick line shows the corresponding result derived from SAGE II zonal mean data over 10°N-S for the same time periods. The dashed line is near the cold point tropopause (17 km).

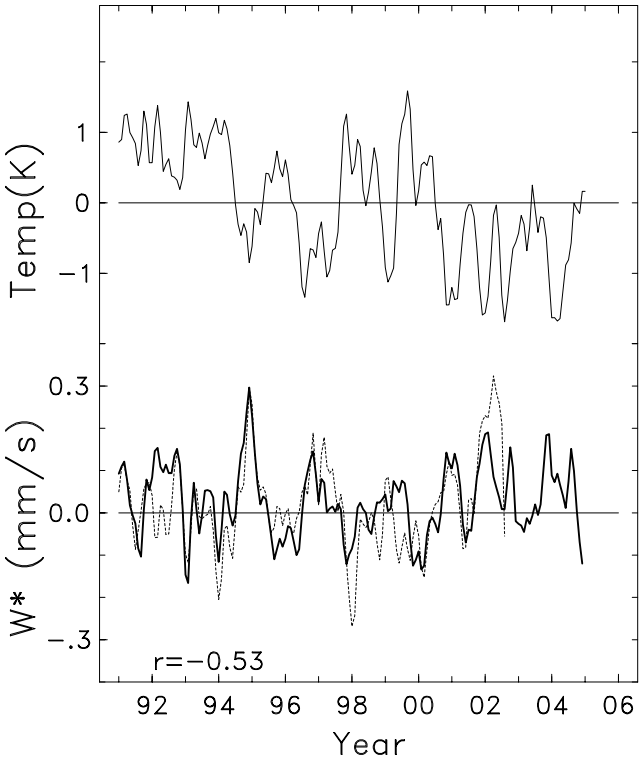

Figure 9. (top) Time series of cold point tropopause temperature anomalies, identical to Figure 4. (bottom) Estimates of interannual variations in tropical vertical velocity at 100 hPa over 20°N–20°S, derived from subtropical momentum balance calculations as discussed in the text. Results are shown on the basis of NCEP (solid line) and ERA40 reanalyses (dashed line).

these in turn result primarily from enhanced momentum flux convergence in the subtropical upper troposphere (noted by the primarily horizontal arrows in Figure 10b). This represents an enhancement of the climatological patterns seen in Figure 10a, i.e., a slight increase in subtropical UTLS momentum fluxes associated with midlatitude baroclinic eddies [e.g., *Trenberth*, 1991]. Analyses of the corresponding zonal mean wind changes for 2001–2004, based on NCEP data, show a weak westerly wind increase (∼0.5–1 m/s) in the tropical UTLS, which represents a slight weakening of the time average easterlies near the equator. The sign of this wind change is consistent with allowing midlatitude eddies to propagate slightly deeper into the tropics [e.g., *Randel and Held*, 1991], qualitatively consistent with the eddy signature in Figure 10b. However, these results should be caveated by the fact that the anomalies are small, and there are known uncertainties and biases in reanalysis data sets [*Santer et al.*, 1999]; note the NCEP temperature data exhibit substantial changes near the tropical tropopause after 2001, probably related to a change in satellite input data (R04). However, while the changes in EP flux and derived upwelling are relatively small, the coherence in time with observed temperature changes (Figure 9) is suggestive that these changes are a real effect.

3.4. Radiative Influence of Tropical Ozone Changes

[19] As discussed above, coupled temperature and ozone changes near the tropical tropopause can result from enhanced upwelling; the coincidence of large responses near ∼15–20 km results from long radiative timescales (for temperature) and strongest background vertical gradients (for ozone). Another mechanism for coupling of ozone and temperature in this region is the radiative response to any ozone changes that occur (for whatever reason). To estimate the importance of this effect, we have calculated the temperature response to an imposed ozone decrease of 10% near the tropical tropopause, with a vertical profile shown in Figure 11 (this is similar to the observed changes in Figure 9). Calculations are based on a fixed dynamical heating radiative transfer model; see *Forster and Joshi* [2005] for details. The resulting radiative temperature changes (also shown in Figure 11) reveal maximum cooling

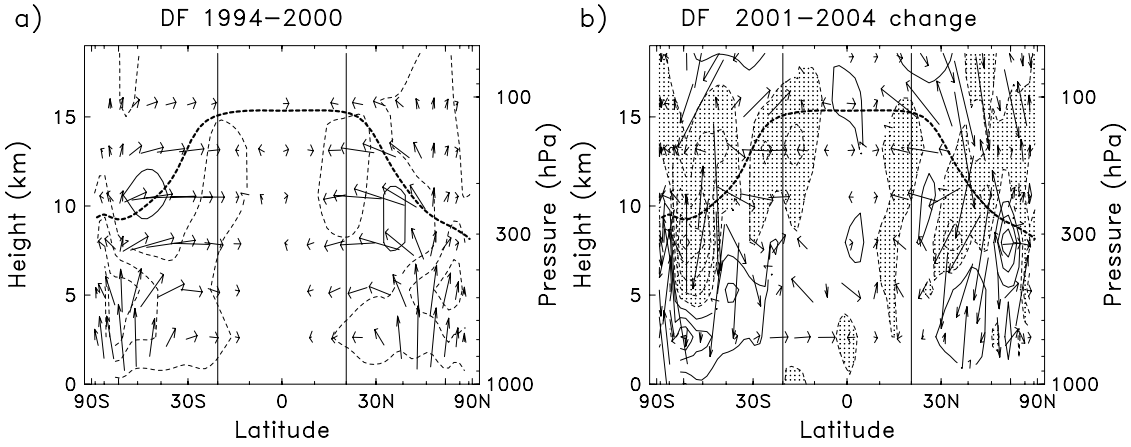

Figure 10. (a) Time average EP flux diagram for the period 1994–2000. Contours show EP flux divergence (wave driving) with values of ±1,3,5, . . . m/s/day. (b) EP flux diagram showing differences between (2001–2004) minus (1994–2000); here contours are ±0.1,0.2,0.3, . . . m/s/day. In each panel the thick dashed line denotes the tropopause, and vertical lines are added at 20°N and 20°S to highlight the latitudes where the tropical upwelling calculations (i.e., Figure 9) are performed. Note the horizontal axes are scaled like sin (latitude), in order to accentuate tropical latitudes.

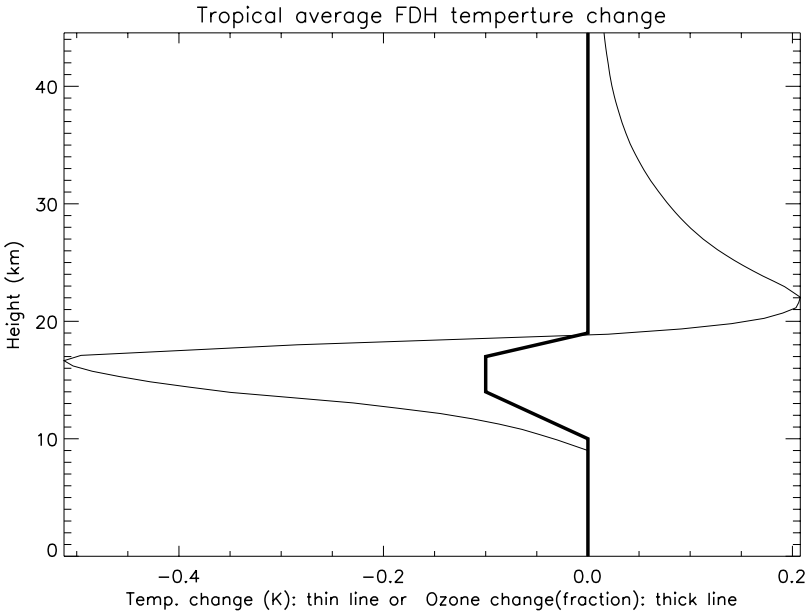

Figure 11. Model calculation of the vertical profile of tropical temperature change (thin line) resulting from an imposed ozone change of −10% near the tropical tropopause (as shown by thick line).

of ∼0.5 K near the tropopause, with a vertical profile similar to the imposed ozone change. Additionally, smaller amplitude warming is found in the lower stratosphere (0.1–0.2 K over 20–27 km), and this is the result of increased upwelling infrared radiation from the troposphere, due to less absorption at the colder tropical tropopause.

[20] The calculated temperature change in Figure 11 (approximately −0.5 K) is a substantial fraction of the observed changes seen in Figure 4, suggesting that the radiative effects of near-tropopause ozone changes could be a relevant factor. This applies to year-to-year variations, and also to long-term decadal changes.

4. Relation to Decadal-Scale Changes

[21] The changes in water vapor, temperature and ozone observed after 2001 dominate the record for the HALOE time period (1992–2005), but it is of interest to understand these changes in the context of longer-term decadal scale variability. Decadal-scale changes for water vapor are poorly understood, as a long record is available from only one station (Boulder, Colorado, for 1980–2005). These data exhibit a long-term increase of ∼1%/year, but there are significant trend differences with HALOE observations for the period after 1992 (as seen in Figure 3). While *Rosenlof et al.* [2001] have combined results from several separate water vapor data sets to suggest a 1% per year global increase over the last several decades, there is currently no explanation for such an increase given observed variability of tropical tropopause temperatures (as discussed by *Fueglistaler and Haynes* [2005]).

[22] Long records of tropical tropopause temperatures derived from historical radiosonde data exhibit cooling trends of order −0.5 K/decade, as shown by *Zhou et al.* [2001] and *Seidel et al.* [2001]. However, detailed comparisons with satellite temperature measurements suggests that radiosonde data at many tropical stations contain artificial cooling biases related to changes (improvements) in instrumentation over time [*Randel and Wu*, 2006]. *Randel and Wu* [2006] have identified a few tropical stations where these biases are relatively small, and Figure 12 shows time series of interannual temperature anomalies at 100 and 70 hPa over 1979–2004 derived from six stations over 20°N-S; note that these data are available for standard pressure levels, and the cold point is not resolved. Time series in Figure 12 show relatively strong decadal-scale cooling for the 70 hPa level (−0.61 ± 0.14 K/decade for 1979–2004,

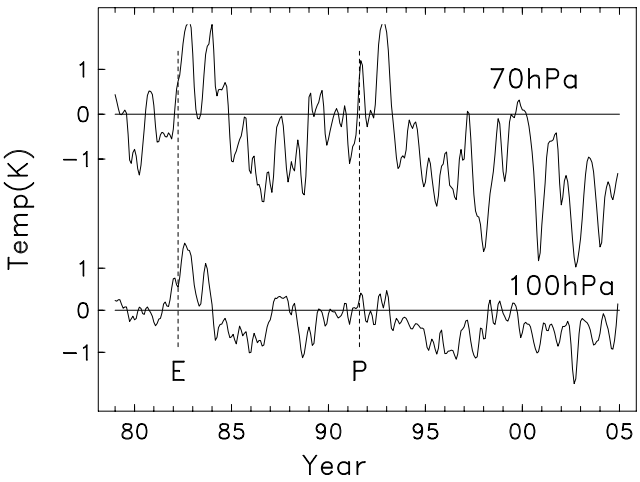

Figure 12. Time series of deseasonalized temperature anomalies at the 100 and 70 hPa levels for 1979–2004, derived from radiosonde measurements at Hilo (20°N), San Juan (18°N), Nairobi (1°S), Manaus (3°S), Townsville (19°S) and Rio de Janiero (23°S). These stations are chosen because of their lack of artificial cooling biases, as discussed in text. E and P denote the volcanic eruptions of El Chichon and Pinatubo, respectively.

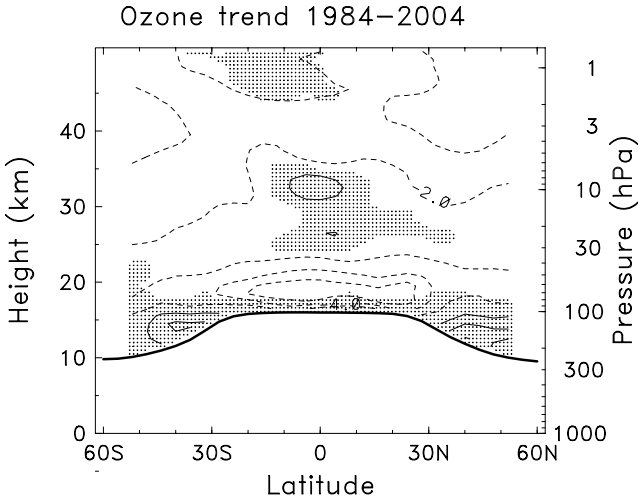

Figure 13. Linear trends in ozone during 1984–2004, derived from SAGE II data. The calculations are based on a standard regression model [*WMO*, 2003]. Contours are 2%/decade, and shading denotes regions where trends are not significant at the 2*sigma level. The thick line denotes the time average tropopause.

calculated neglecting volcanic time periods), with markedly cold anomalies over the last several years (consistent with the cold point time series in Figure 4). The time series at 100 hPa show relatively less long-term cooling (-0.19 ± 0.07 K/decade). These data suggest there has been some substantial decadal-scale cooling of the tropopause region, which lies between the 100–70 hPa levels. These trends have been accelerated because of the recent cold anomalies, especially at the 70 hPa level. We note that these tropical cooling trends are qualitatively similar to those discussed by *Thompson and Solomon* [2005], although the magnitude of the changes and the detailed spatial structure is different, on the basis of this subset of the LKS+IGRA data.

[23] Estimates of long-term trends in ozone near the tropical tropopause rely completely on satellite data, as the ozonesonde record is poor prior to the SHADOZ network beginning in 1998. Figure 13 shows trend calculations for the SAGE II data for the period 1984–2004, and these highlight relatively large negative trends in the tropical tropopause region of approximately −5%/decade. These derived trends are significantly influenced by the ozone decreases after 2001, which occur at the end of the record (as seen in Figure 7); however, negative ozone trends in this region have been seen in previous analyses of SAGE data [*World Meteorological Organization* (*WMO*), 2003, Figure 4–10].

[24] In summary, the results here show decadal-scale decreases in temperature and ozone near the tropical tropopause that are similar to, and in fact strongly influenced by, the changes observed since 2001. Calculations of derived upwelling at 100 hPa based on NCEP reanalysis data (as in Figure 9) do not show significant trends for 1979–2004, although there are many uncertainties in such highly derived calculations. In this regard, we note that the model simulations of *Buchart and Scaife* [2001] suggest increases in tropical stratospheric upwelling in a future changing climate, but the calculated increase is only ∼3%/decade, which is small compared to the ∼10% year-to-year changes evident in Figure 9.

5. Summary and Discussion

[25] Global satellite observations from HALOE show a substantial, persistent decrease in stratospheric water vapor since 2001. These low values originate near the tropical tropopause, and propagate coherently in latitude and height to cover most of the global stratosphere (R04). Independent measurements of stratospheric water vapor from balloon observations at Boulder, Colorado (40°N) and POAM III satellite data over the Arctic (∼55–70°N) show decreases after 2001, consistent with the HALOE data. Time series of tropical tropopause temperatures are strongly correlated with the stratospheric water vapor changes, and in particular there have been anomalously cold tropopause temperatures for the period 2001–2004. The temperature changes are quantitatively consistent with the magnitude of water vapor changes. The spatial structure of the temperature changes for 2001–2004 show cold anomalies of order 1 K over a narrow vertical layer (∼15–20 km) near the tropopause (Figure 4). The temperature changes are largest in equatorial latitudes, and are evident over all longitudes.

[26] We have also examined changes in the vertical profile of ozone in the tropics, on the basis of ozonesonde observations from SHADOZ (covering 1998–2004) and SAGE II satellite data (for 1984–2004). Both sets of observations show a decrease in ozone near the tropopause after 2001, with similar temporal behavior to the temperature and water vapor changes. There is remarkably good agreement between the averaged SHADOZ data and zonal mean SAGE II time series, both for the detailed time variation of ozone (Figure 7) and the profile of ozone changes (Figure 8). The spatial structure of ozone changes for 2001–2004 shows percentage decreases of ∼10% near and above the tropical tropopause (∼15–20 km), primarily over equatorial latitudes. Notably, the ozone changes are evident over a wide range of longitudes, even over regions far from chronic deep convection (e.g., San Cristobal in the eastern Pacific Ocean). Overall, the tropical ozone changes for 2001–2004 have similar characteristics to the observed temperature changes, and they appear coupled.

[27] The coupled ozone-temperature decreases near the tropopause could possibly result from several mechanisms, including (1) an increase in the mean upwelling circulation and (2) a systematic increase in tropical deep convection, or a combination of these effects. Part of the tropical cooling would likely result from a radiative response to the ozone decreases, of whatever cause.

[28] Tropical deep convection can influence both temperature and ozone near the tropical tropopause [e.g., *Kuang and Bretherton*, 2004; *Folkins et al.*, 2002], and systematic increases in deep convection could potentially lead to tropopause cooling and ozone decreases. It is difficult to quantify systematic long-term changes in tropical deep convection based on satellite measured outgoing longwave radiation (OLR), because of changes in operational satellites and drifting equatorial crossing times [*Lucas et al.*, 2001]. However, several features of the observed temperature-ozone changes suggest that deep convection is not the primary cause. Both temperature and ozone changes occur

over a wide range of longitudes, rather than localized over regions of persistent deep convection (e.g., the tropical western Pacific); note especially that substantial ozone decreases for 2001–2004 are observed at San Cristobal and Nairobi. Furthermore, tropical deep convection most strongly influences ozone profiles below ~14 (or at most 16) km, associated with the main convective outflow layer [*Folkins et al.*, 2002; *Solomon et al.*, 2005], whereas the observed ozone changes occur at higher altitudes up to ~20 km (Figure 8). These characteristics argue against systematic changes in deep convection as a primary cause of the observed temperature and (especially) ozone changes.

[29] A more likely mechanism for the coupled ozone-temperature changes is an increase in the mean tropical upwelling circulation. Such an increase in upwelling would explain the longitudinal symmetry and maximum changes near the equator for both temperature and ozone. Furthermore, the observed vertical structure of maximum changes near the tropopause (~15–20 km) can be explained by the coincidence of long radiative relaxation timescales in this region (which enhances low-frequency temperature response), and strongest fractional vertical gradient for ozone (so that the fractional ozone response to upwelling is magnified). Thus the maximum changes for both temperature and ozone near the tropical tropopause are consistent with an enhanced tropical upwelling (Brewer-Dobson) circulation.

[30] On the basis of this reasoning, we have examined circulation statistics to search for evidence of an increased Brewer-Dobson circulation. Tropical upwelling can be estimated by diagnostic analyses of the subtropical momentum budget, combined with continuity [*Rosenlof*, 1995]. We have used such calculations to evaluate interannual changes in upwelling $\langle \overline{w}^*_m \rangle$ that are in balance with variations in the momentum forcing over 20°N–20°S. Such calculations are in general very sensitive to data details, because of uncertainties in estimating EP flux divergence in the subtropical tropopause region (weighted by the inverse Coriolis parameter). Nonetheless, we find significant anticorrelation between derived $\langle \overline{w}^*_m \rangle$ and tropopause temperature anomalies during 1993–2004 (Figure 9), and also reasonable agreement between $\langle \overline{w}^*_m \rangle$ estimates from NCEP and ERA40 data sets. Anomalies in $\langle \overline{w}^*_m \rangle$ show enhanced upwelling during 2001–2004, consistent with cold tropopause temperatures and reduced ozone. On the basis of the NCEP data, the cause of the stronger upwelling after 2001 is a slight increase in EP flux divergence in the subtropical UTLS region (Figure 10b), associated with enhanced momentum flux convergence from subtropics (in both hemispheres).

[31] Another mechanism that contributes to ozone-temperature coupling is the direct radiative response to ozone change, in this case a cooling coincident with decreased ozone near the tropopause. We have estimated the magnitude of this effect using a fixed dynamical heating radiative calculation, and the results show that a 10% ozone loss near the tropopause results in a coincident cooling of ~0.5 K. This is a substantial fraction of the observed temperature changes for 2001–2004, and this mechanism acts to reinforce the dynamically coupled ozone-temperature changes. We note that such ozone feedbacks could also be relevant for understanding the seasonal cycle in temperature near the tropical tropopause.

[32] Overall the observations here paint a reasonably coherent picture of increased subtropical EP fluxes leading to enhanced tropical upwelling, which in turn lead to lower ozone, colder temperature and corresponding lower-stratospheric water vapor. While the overall changes in most quantities are small, the end effect on water vapor is substantial, with decreases of order 10% background values (Figures 1 and 2). The changes in water vapor furthermore propagate to cover much of the stratosphere, so that a linkage between tropical upwelling, subtropical UTLS EP fluxes and the global stratosphere is observed. Such a linkage is clearly observed for the large seasonal cycle in circulation, temperature and constituents near the tropical tropopause, and the interannual changes observed here are a reasonable extension of those links.

[33] Analysis of longer-term records show decadal-scale decreases in temperature and ozone near the tropical tropopause that are similar to, and in fact strongly influenced by, the changes observed since 2001. We note that the 25- or 20-year records in Figures 12 and 13 are relatively short and strongly influenced by end values, and it is unclear if the recent changes reflect low-frequency natural variability or an accentuation and continuation of monotonic trends.

[34] **Acknowledgments.** We thank several people for discussions and comments on this work, including Rolando Garcia, Andrew Gettelman, J.F. Lamarque, Warwick Norton, Karen Rosenlof, James M. Russell III and Kevin Trenberth. This work is partially supported by the NASA ACMAP program. The National Center for Atmospheric Research is sponsored by the National Science Foundation.

References

Angell, J. K. (1997), Stratospheric warming due to Agung, El Chichon and Pinatubo taking into account the quasi-biennial oscillation, *J. Geophys. Res.*, *102*, 9479–9485.

Avallone, L. M., and M. J. Prather (1996), Photochemical evolution of ozone in the tropical lower stratosphere, *J. Geophys. Res.*, *101*, 1457–1461.

Brewer, A. W. (1949), Evidence for a world circulation provided by measurements of helium and water vapor distribution in the stratosphere, *Q. J. R. Meteorol. Soc.*, *75*, 351–363.

Buchart, N., and A. Scaife (2001), Removal of chlorofluorocarbons by increased mass exchange between the stratosphere and troposphere in a changing climate, *Nature*, *410*, 799–802.

Chiou, E. W., L. W. Thomason, and W. P. Chu (2006), Variability of stratospheric water vapor inferred from SAGE II, HALOE and Boulder balloon measurements, *J. Clim.*, in press.

Dessler, A. E. (2002), The effect of deep, tropical convection on the tropical tropopause layer, *J. Geophys. Res.*, *107*(D3), 4033, doi:10.1029/2001JD000511.

Folkins, I., C. Braun, A. M. Thompson, and J. Witte (2002), Tropical ozone as an indicator of deep convection, *J. Geophys. Res.*, *107*(D13), 4184, doi:10.1029/2001JD001178.

Forster, P. M. de F., and M. Joshi (2005), The role of halocarbons in the climate change of the troposphere and stratosphere, *Clim. Change*, *71*, 249–266.

Fueglistaler, S., and P. H. Haynes (2005), Control of interannual and longer-term variability of stratospheric water vapor, *J. Geophys. Res.*, *110*, D24108, doi:10.1029/2005JD006019.

Fueglistaler, S., M. Bonazzola, P. Haynes, and T. Peter (2005), Stratospheric water vapor predicted from the Lagrangian temperature history of air entering the stratosphere in the tropics, *J. Geophys. Res.*, *110*, D08107, doi:10.1029/2004JD005516.

Geller, M. A., X. Zhou, and M. Zhang (2002), Simulations of the interannual variability of stratospheric water vapor, *J. Atmos. Sci.*, *59*, 1076–1085.

Giorgetta, M. A., and L. Bengston (1999), Potential role of the quasi-biennial oscillation in the stratosphere-troposphere exchange as found in water vapor in general circulation model experiments, *J. Geophys. Res.*, *104*, 6003–6019.

Harries, J. E., et al. (1996), Validation of measurements of water vapor from the Halogen Occultation Experiment, HALOE, *J. Geophys. Res.*, *101*, 10,205–10,216.

Haynes, P. H., C. J. Marks, M. E. McIntyre, T. G. Shepherd, and K. P. Shine (1991), On the 'downward control' of extratropical diabatic circulations by eddy-induced zonal mean forces, *J. Atmos. Sci.*, *48*, 651–678.

Holton, J. R., P. Haynes, M. McIntyre, A. Douglass, R. Rood, and L. Pfister (1995), Stratosphere-troposphere exchange, *Rev. Geophys.*, *33*, 403–439.

Kalnay, E., et al. (1996), The NCEP/NCAR reanalysis project, *Bull. Am. Meteorol. Soc.*, *77*, 437–471.

Kerr-Munslow, A. M., and W. Norton (2006), Tropical wave driving of the annual cycle in tropopause temperatures, Part 1: ECMWF analyses, *J. Atmos. Sci.*, *63*, 1419–1419.

Kuang, Z., and C. S. Bretherton (2004), Convective influence on the heat balance of the tropical tropopause layer: A cloud-resolving model study, *J. Atmos. Sci.*, *61*, 2919–2927.

Lanzante, J., S. Klein, and D. J. Seidel (2003a), Temporal homogenization of monthly radiosonde temperature data. Part I: Methodology, *J. Clim.*, *16*, 224–240.

Lanzante, J., S. Klein, and D. J. Seidel (2003b), Temporal homogenization of monthly radiosonde temperature data. Part II: Trends, sensitivities and MSU comparisons, *J. Clim.*, *16*, 241–262.

Lucas, L. E., D. E. Waliser, J. E. Janowiak, and B. Liebman (2001), Removing the satellite equatorial crossing time biases from the daily outgoing longwave radiation data set, *J. Clim.*, *14*, 2583–2605.

McCormick, M. P., J. M. Zawodny, R. E. Viega, J. C. Larsen, and P. H. Wang (1989), An overview of SAGE I and II ozone measurements, *Planet. Space Sci.*, *37*, 2157–2186.

Mote, P. W., K. H. Rosenlof, J. R. Holton, R. S. Harwood, and J. W. Waters (1996), An atmospheric tape recorder: The imprint of tropical tropopause temperatures on stratospheric water vapor, *J. Geophys. Res.*, *101*, 3989–4006.

Nedoluha, G. E., R. M. Bevilacqua, K. W. Hoppel, J. D. Lumpe, and H. Smit (2002), Polar Ozone and Aerosol Measurement III measurements of water vapor in the upper troposphere and lowermost stratosphere, *J. Geophys. Res.*, *107*(D10), 4103, doi:10.1029/2001JD000793.

Oltmans, S. J., H. Vomel, D. J. Hofmann, K. Rosenlof, and D. Kley (2000), Increases in stratospheric water vapor from balloon borne frostpoint hygrometer measurements at Washington, D. C., and Boulder, Colorado, *Geophys. Res. Lett.*, *27*, 3453–3456.

Plumb, R. A., and J. Eluszkiewicz (1999), The Brewer-Dobson circulation: Dynamics of the tropical upwelling, *J. Atmos. Sci.*, *56*, 868–890.

Randel, W. J., and I. M. Held (1991), Phase speed spectra of transient eddy fluxes and critical layer absorption, *J. Atmos. Sci.*, *48*, 688–697.

Randel, W. J., and F. Wu (2006), Biases in stratospheric and tropospheric temperature trends derived from historical radiosonde data, *J. Clim.*, *19*, 2094–2104.

Randel, W. J., R. R. Garcia, and F. Wu (2002), Time-dependent upwelling in the tropical lower stratosphere estimated from the zonal-mean momentum budget, *J. Atmos. Sci.*, *59*, 2141–2152.

Randel, W. J., F. Wu, S. J. Oltmans, K. Rosenlof, and G. Nedoluha (2004), Interannual changes of stratospheric water vapor and correlations with tropical tropopause temperatures, *J. Atmos. Sci.*, *61*, 2133–2148.

Rosenlof, K. H. (1995), Seasonal cycle of the residual mean meridional circulation in the stratosphere, *J. Geophys. Res.*, *100*, 5173–5191.

Rosenlof, K. H., et al. (2001), Stratospheric water vapor increases over the past half-century, *Geophys. Res. Lett.*, *28*, 1195–1198.

Russell, J. M., III, A. F. Tuck, L. L. Gordley, J. H. Park, S. R. Drayson, J. E. Harries, R. J. Cicerone, and P. J. Crutzen (1993), The Halogen Occultation Experiment, *J. Geophys. Res.*, *98*, 10,777–10,797.

Santer, B. D., et al. (1999), Uncertainties in observationally based estimates of temperature change in the free atmosphere, *J. Geophys. Res.*, *104*, 6305–6334.

Seidel, D. J., R. J. Ross, J. K. Angell, and G. C. Reid (2001), Climatological characteristics of the tropical tropopause as revealed by radiosondes, *J. Geophys. Res.*, *106*, 7857–7878.

Solomon, S., D. W. J. Thompson, R. W. Portmann, S. J. Oltmans, and A. M. Thompson (2005), On the distribution and variability of ozone in the tropical upper troposphere: Implications for tropical deep convection and chemical-dynamical coupling, *Geophys. Res. Lett.*, *32*, L23813, doi:10.1029/2005GL024323.

Thompson, A. M., et al. (2003), Southern Hemisphere Additional Ozonesondes (SHADOZ) 1998–2000 tropical ozone climatology: 1. Comparison with Total Ozone Mapping Spectrometer (TOMS) and ground-based measurements, *J. Geophys. Res.*, *108*(D2), 8238, doi:10.1029/2001JD000967.

Thompson, D. W. J., and S. Solomon (2005), Recent stratospheric climate trends: Global structure and tropospheric linkages, *J. Clim.*, *18*, 4785–4795.

Trenberth, K. E. (1991), Storm tracks in the Southern Hemisphere, *J. Atmos. Sci.*, *48*, 2159–2178.

Volk, C. M., et al. (1996), Quantifying transport between the tropical and mid-latitude lower stratosphere, *Science*, *272*, 1763–1768.

World Meteorological Organization (2003), Scientific Assessment of Ozone Depletion: 2002, *Global Ozone Res. Monit. Proj. Rep. 47*, Geneva, Switzerland.

Zhou, X. L., M. A. Geller, and M. Zhang (2001), Cooling trend of the tropical cold point tropopause temperatures and its implications, *J. Geophys. Res.*, *106*, 1511–1522.

P. Forster, School of Earth and Environment, University of Leeds, Leeds LS2 9JT, UK.

G. E. Nedoluha, Naval Research Laboratory, Washington, DC 20375, USA.

W. J. Randel and F. Wu, National Center for Atmospheric Research, Boulder, CO 80307, USA. (randel@ucar.edu)

H. Vömel, Global Monitoring Division, NOAA Earth System Research Laboratory, Boulder, CO 80305, USA.